Carbohydrate Polymers 110 (2014) 121–127

Contents lists available at ScienceDirect

Carbohydrate Polymers

journal homepage: www.elsevier.com/locate/carbpol

Study on novel functional materials carboxymethyl cellulose lithium (CMC-Li) improve high-performance lithium-ion battery

Lei Qiu, Ziqiang Shao*, Pan Xiang, Daxiong Wang, Zhenwen Zhou, Feijun Wang, Wenjun Wang, Jianquan Wang

College of Material Science and Engineering, Beijing Institute of Technology, Beijing Engineering Technology Research Centre for Cellulose and Its Derivative Materials, Beijing 100081, PR China

ARTICLE INFO

Article history:
Received 20 February 2014
Received in revised form 8 March 2014
Accepted 20 March 2014
Available online 28 March 2014

Keywords:
Lithium battery
$LiFePO_4$
Cellulose derivative
CMC-Li
Electrospinning

ABSTRACT

Novel cellulose derivative CMC-Li was synthesized by cotton as raw material. The mechanism of the CMC-Li modified electrode materials by electrospinning was reported. CMC-Li/lithium iron phosphate ($LiFePO_4$, LFP) composite fiber coated with LFP and CMC-Li nanofibers was successfully obtained by electrospinning. Then, CMC-Li/LFP nano-composite fiber was carbonized under nitrogen at a high temperature formed CNF/LFP/Li (CLL) composite nanofibers as cathode material. It can increase the contents of Li^+, and improving the diffusion efficiency and specific capacity. The battery with CLL as cathode material retained close to 100% of initial reversible capacity after 200 cycles at 168 mAh g^{-1}, which was nearly the theoretical specific capacity of LFP. The cyclic voltammetry (CV), electrochemical impedance spectroscopy (EIS), X-ray diffraction (XRD) and scanning electron microscope (SEM) were characterizing material performance. The batteries have good electrochemical property, outstanding pollution-free, excellent stability.

1. Introduction

Lithium batteries, as a main power source or back-up power source for mobile communication devices (Gur, Sawyer, & Prasher, 2012), portable electronic devices and the like (Cheng & Fan, 2012; Xiong, Tang, Wang, & Pan, 2014), have received increasing attention in the scientific and industrial fields due to their high electromotive force and high-energy density (Wang & Wan, 2011; Yang et al., 2011; Yuan, Xu, & Mueller, 2011). To meet the demand for the higher-energy density and improved cycle characteristics of batteries, a great deal of attempt has been made to design new structures of electrode materials and develop new electrode materials in recent years (Dimesso et al., 2012; Stein, 2011). LFP is one of the ideal cathode materials for power and energy storage lithium-ion battery at present as its advantage of superior safety property, long cycle life, wide raw material source, no environmental pollution and so on (Janssen et al., 2013; Malik, Zhou, & Ceder, 2011). It has been a hot topic of research and development of cathode materials for lithium-ion battery (Hu, Wu, Lin, Khlobystov, & Li, 2013; Kuss, Lepage, Liang, & Schougaard, 2013). Since the electrical conductivity of LFP was an extremely low, and diffusion coefficient of Li^+ was small, which led to the result in poor property of the rate of charge and discharge (Sasaki, Ukyo, & Novak, 2013). With the increase of the current density of charge and discharge, there was the phenomenon of capacity of rapid decay. The methods of surface coating (Qiu, Shao, Yang, et al., 2013), dispersing electronic conductor (Jiang, Duan, Schobel, Agarwal, & Greiner, 2013; Marcicki, Canova, Conlisk, & Rizzoni, 2013), ion doping (Gibot et al., 2008; Petrovic et al., 2013) had a better effect on increasing the conductivity. It not only improved conductivity between the particles, enhanced internal conductivity of LFP particles, and provided an electronic channel for LFP, but also reduced the polarization of the battery. The particle size of LFP in electrode material was the key to improving diffusion capacity of Li^+ in LFP, and its application of electrospinning provided a better way for such study (Wu et al., 2013).

Cotton, for the first of time, as a raw material and further synthesized CMC-Li by a unique two-step method (Qiu, Shao, Wang, Zhang, & Cao, 2013). This polymer with a unique molecular structure is a polyhydroxy water soluble derivative polymer. Since it is difficult to find a solvent suitable for water-soluble polysaccharide ionic polymer to be electrospun at present, thus the study on electrospinning for water soluble ionic cellulose ether is always a

* Corresponding author. Tel.: +86 10 68940942; fax: +86 10 68941797.
E-mail addresses: qiulei1010@126.com (L. Qiu), shaoziqiang409@163.com (Z. Shao).

http://dx.doi.org/10.1016/j.carbpol.2014.03.052
0144-8617/

problem in the related field, especially, it is a blank in the study on electrospinning for CMC-Li (Rodriguez, Gatenholm, & Renneckar, 2012). And based on a large number of experiments, for the first time, we proposed an electrospinning method suitable for water soluble ionic cellulose ether CMC-Li (Qiu, Shao, Yang, et al., 2014). Then we obtained CMC-Li nanofiber by electrospinning, and further studied on the functionalization of fiber material, which broke through the difficulty in related research. This study has the following important implications, the polysaccharide ionic polymer nanofibers was prepared by electrospinning, and it can also provide a good idea for scholars who specialized in water soluble film materials, tissue engineer scaffold materials and biological medicine embedding materials (Blachechen, Souza, & Petri, 2012; Ritcharoen et al., 2008). We also found that CMC-Li with low molecular weight is suitable for functionalizing by electrospinning. And high molecular weight can result in large polymer viscosity and tension of the liquid surface, which causes the spinning process to be more difficult (Qiu, Shao, Liu, et al., 2014).

In our work, for the first time, we used cotton as raw material and then successfully synthesized CMC-Li products with different DS and molecular weight. Next, CMC-Li/LFP composite fiber coated with LFP and CMC-Li nanofibers were successfully obtained by electrospinning, LFP was uniformly distributed in fibers. CMC-Li was applied to modify lithium battery electrode materials by electrospinning. Then, CMC-Li/LFP nano-composite fiber was carbonized under nitrogen at a high temperature, after that, it not only obtained the modified LFP electrode material with uniform carbon coating, namely CNF/LFP, but also increased the contents of Li-ions in electrode material and formed CNF/LFP/Li (CLL) composite nanofibers as cathode material. Finally, we used CLL and unmodified LFP as cathode material of battery, respectively, PVDF as a binder to assemble button battery for the performance testing and comparing. This unique method not only meets the demand for carbonizing and modifying electrode material by electrospinning, but also uniquely increased contents of freely moving lithium ion in electrode material and the efficiency of prolapsing and embedding of lithium ion between cathode and anode electrode. C, Li^+ and electrode material formed fully stable network structure model. Thus improving the charge and discharge capacity of the whole lithium-ion battery.

2. Experimental

2.1. Materials

Purified cotton (M100) was supplied by Xi' An North Hui Chemical Industry Co., Ltd. (Xi' An, China). Monochloroacetic acid, glacial acetic acid, sulfuric acid (98% solution), ethanol (EtOH) was supplied by Beijing Chemical fine Chemical Co., Ltd. (Beijing, China). Polyethylene oxide (PEO), lithium hydroxide monohydrate ($LiOH{\cdot}H_2O$) were supplied by Alfa Aesar Chemical Co., Ltd. (Tianjin, China). $LiFePO_4$ was kindly supplied by Shanxi Power source Co., Ltd. (Taiyuan, Shanxi, China).

2.2. CMC-Li powder preparation

The preparation process of CMC-Li can be made clear by the slurry process in a solution of isopropyl alcohol in our laboratory (Qiu, Shao, Wang, et al., 2013). CMC-Lis with the different degree of substitution (DS) were prepared by selecting the DS of CMC-Na and the amount of $LiOH{\cdot}H_2O$. In this paper, CMC-Lis with three different DS values were prepared, CMC-Li-1 (DS = 0.62, Mw = 900 g mol^{-1}), CMC-Li-2 (DS = 0.84, Mw = 2500 g mol^{-1}), CMC-Li-3 (DS = 1.20, Mw = 4300 g mol^{-1}).

2.3. Electrospinning

CMC-Lis were dissolved in a mixed solvent of water, and a small amount of PEO (c = 2 wt%) was added to obtain the solution. LFP was added to solvent, and then intermittent ultrasound concussion was carried out 10 min later. CMC-Li was completely dissolved and poured into the needle. The processing conditions were adjusted at a flow rate of 4 ml/h, with an applied voltage of 25 kV, at a capillary tip-to-target distance of 10 cm and a temperature of 25 °C, and nano-CMC-Li fiber and CMC-Li/LFP fiber were obtained by an electrospinning device.

2.4. Structural characterization and electrochemical measurements

XRD diffraction experiments were performed with a Inel Cps 300 diffracts meters using the Cu Kα radiation (λ = 1.54056 Å). Morphology and structure of electrospun CMC-Li fibers were observed with a SEM, JSM-6700F after gold coating. CV and EIS results were obtained with electrochemical workstation CHI660E from Shanghai Chen Hua Instruments Co., Ltd. The coin cells (CR2025) were assembled to test the electrochemical performance of the as-prepared CLL (or LFP):acetylene black:PVDF is 80:10:10, using 1 M $LiPF_6$EC/DEC/DMC (1:1:1 by volume) as the electrolyte and a Li foil as the counter electrode. The cells were charged and discharged galvanostatically in the fixed potential window from 2.0 to 4.2 V on a Shenzhen Neware battery cycle (China) at 25 °C. The calculated capacity was based on the whole mass of the cathode electrodes. CV was conducted in a cell at 0.1 mV s^{-1} and performed from 4.2 V to 2.0 V. EIS was measured by applying an alternating potential of 5 mV over the frequency ranging from 10^{-1} to 10^5 Hz after five cycles.

3. Results and discussion

3.1. The preliminary investigation of the mechanism of the CNF/LFP/Li

We used cotton as raw material and then successfully synthesized CMC-Li products with different DS and molecular weight (Figs. S1 and S2). Next, CMC-Li/LFP composite fiber coated with LFP and CMC-Li nanofibers were successfully obtained by electrospinning. LFP was uniformly distributed in fibers. Then, CMC-Li/LFP nano-composite fiber was carbonized under nitrogen at a high temperature, after that, it not only obtained the modified LFP electrode material with uniform carbon coating, namely CNF/LFP, but also increased the contents of Li-ions in electrode material and formed CLL composite nanofibers as cathode material (Fig. 1). CMC-Li could be ascribed to strong hydrogen bonds resulting from the action of the —OH groups, which contributed to the formation of an efficient network (Ryou et al., 2013). Sintering of the electrospun nanofiber not only removes the polymeric precursor backbone but also crystallizes the LFP nanoparticles. We propose the formation mechanism of electrospun LFP nanotubes in which partially crystallized individual LFP nanoparticles from the building blocks that self-assemble and inter-grow into a continuous fibrous morphology after the removal of volatile species at 600 °C for 2 h. If the weight ratio of CMC-Li in the electrospinning solution is higher than the metal ions, the fibers break into several segments of shorter nanofiber (CNF/LFP/Li) due to the drastic structural changes when the CMC-Li backbone is heated. On the other hand, reducing the amount of CMC-Li, results in the closer dispersion of the individual LFP nanoparticles that tend to self-aggregate to construct long continuous fibers (LFP/CNF) upon sintering. Higher DS of CMC-Li, the more freely moving lithium ion was provided with battery. Finally,

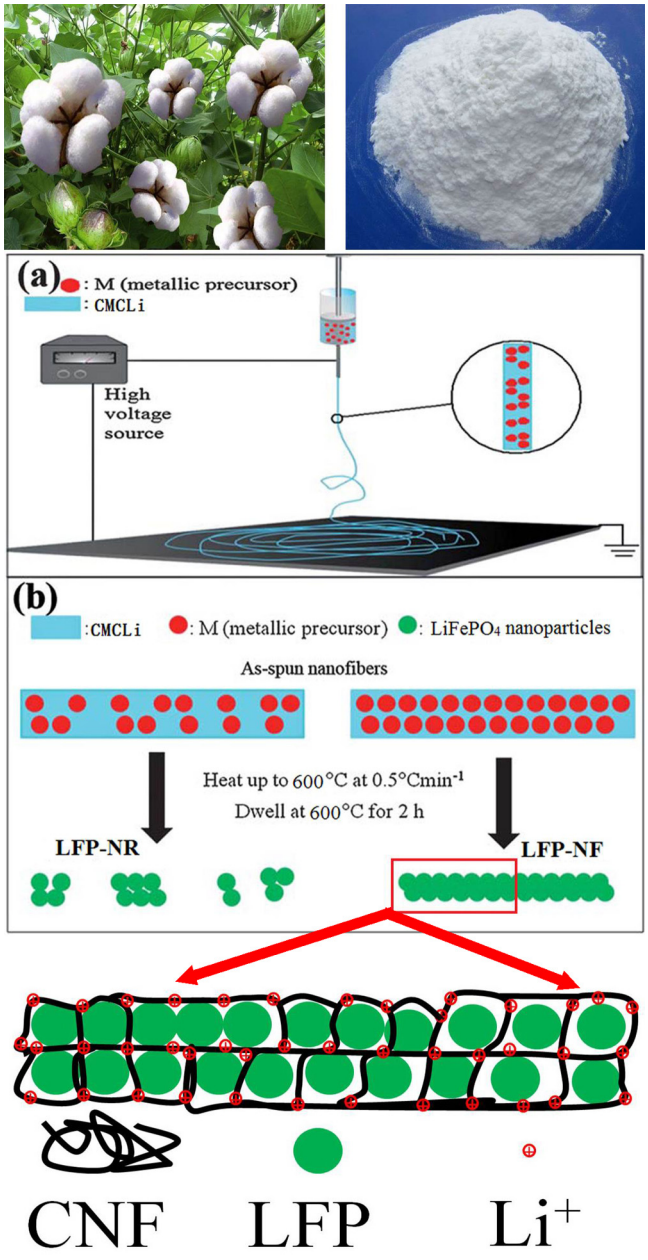

Fig. 1. Schematic illustration of assembling battery. (a) The magnified details of as-spun fibers which consist of CMC-Li as the polymer agent and dispersed LFP nanoparticles. (b) Mechanism of formation of CMC-Li/LFP and CLL electrospun nanofibers has been proposed.

we used CLL and unmodified LFP as cathode material of battery, respectively, and PVDF as a binder to assemble 2025 button battery for the performance testing and comparing.

3.2. SEM photos of composite nanofibers

The particle of unmodified LFP electrode material was smaller, and some particle was gathering (Fig. 2a). CMC-Li nanofiber was successfully obtained by electrospinning (Fig. 2b). It can be seen that the surface of the fiber was relatively smooth, and the diameter was small and about 90 nm. The dispersion was relatively uniform, and there was no formation of the larger links or particularly of messy breakpoints. All of these proved that the spinning process was more stable, and laying a good foundation for studying on functional water soluble ionic polymer materials by electrospinning. The particle of LFP was uniformly dispersed in fibers (Fig. 2c), and formed the CMC-Li/LFP composite nanofiber with excellent morphology and structure. Under the protection of nitrogen, the composite fiber was carbonized at a high temperature (600 °C) to obtain CLL composite fiber (Fig. 2d). The CLL maintained the skeleton structure of nanofiber, and the particle of LFP was more uniformly distributed and coated with carbon nanofiber. The combination was better among carbon, LFP, Li-ion, and a study is being conducted with CLL as cathode material in lithium battery.

3.3. Analysis of precursor TG-DSC at the different temperatures

Fig. 3 showed that the evaporation of water began to be prolapsed and cellulose derivatives began to be dissolved in the weightlessness interval of range from room temperature to 220 °C. When the temperature was increased from 220 °C to 600 °C, organic polymer CMC-Li began to be dissolved by heat. With the maximum exothermic peak and the weight loss process appearing in this temperature range, the weight loss rate of CMC-Li is fastest at 260–300 °C, namely, the main pyrolysis range. In this process, it was well known by the DSC diagram that there was an exothermic peak in the place of 285 °C, which may correspond to the decomposition of organic polymer CMC-Li. Then the temperature continued to increase, and the remaining CMC-Li existing as in the form of carbonaceous residue and lithium salt, and weightlessness became slower. After 600 °C, it began to go into a state of constant weight, and only LFP was generated. We can be clear from the above analysis that the sintering temperature should be at least above 600 °C in order to obtain the well crystallized LFP.

3.4. X-ray diffraction crystal structure of electrode materials

In the XRD chart of the electrode slices with PVDF as binder, CLL as cathode material, in addition to completely include the standard XRD peak of LFP, there was XRD peak of Li, and it was more prominent in the crystal plane (2 1 1) (Moriwake et al., 2013). All of these showed that CMC-Li modified cathode material maybe to increase the contents of lithium ions in the entire battery, and improve the efficiency of prolapsing and embedding of lithium ions between cathode and anode electrode, thus, improving the diffusion efficiency and specific capacity (Fig. 4).

3.5. The curve analysis of the cycle life with different materials

In our experiment, CMC-Li with different DS was electrospun to obtain different CLL as cathode material for lithium-ion battery, and combined with PVDF to assemble button batteries, which were compared with performance of button battery assembled by unmodified LFP as cathode material. It is found that the first charge and discharge specific capacity of batteries using CLL as cathode material was higher than that using unmodified LFP as cathode materials. Among them, the highest one is the battery with CLL-3 as an electrode material, and the value reached 168 mAh g^{-1} and 161 mAh g^{-1}, respectively, which was improved by 15.1% and 11.8% than which with unmodified LFP as electrode material. Moreover, the first charge and discharge loss was only 4.1%. Meantime, the charge and discharge platform are high, which showed that it enhanced the conductivity of cathode materials, shortened the diffusion path of Li-ion, reduced the degree of polarization between the electrodes and increased electrochemical performance. After 200 cycles, specific capacity loss of battery with CLL as electrode material was less than that with unmodified LFP as electrode material when the cycle efficiency was nearly 100%. Among them, the least one is the battery with CLL-3 as electrode material, which is almost close to zero and has the best performance. All of these proved that the unique method using CMC-Li to modify electrode

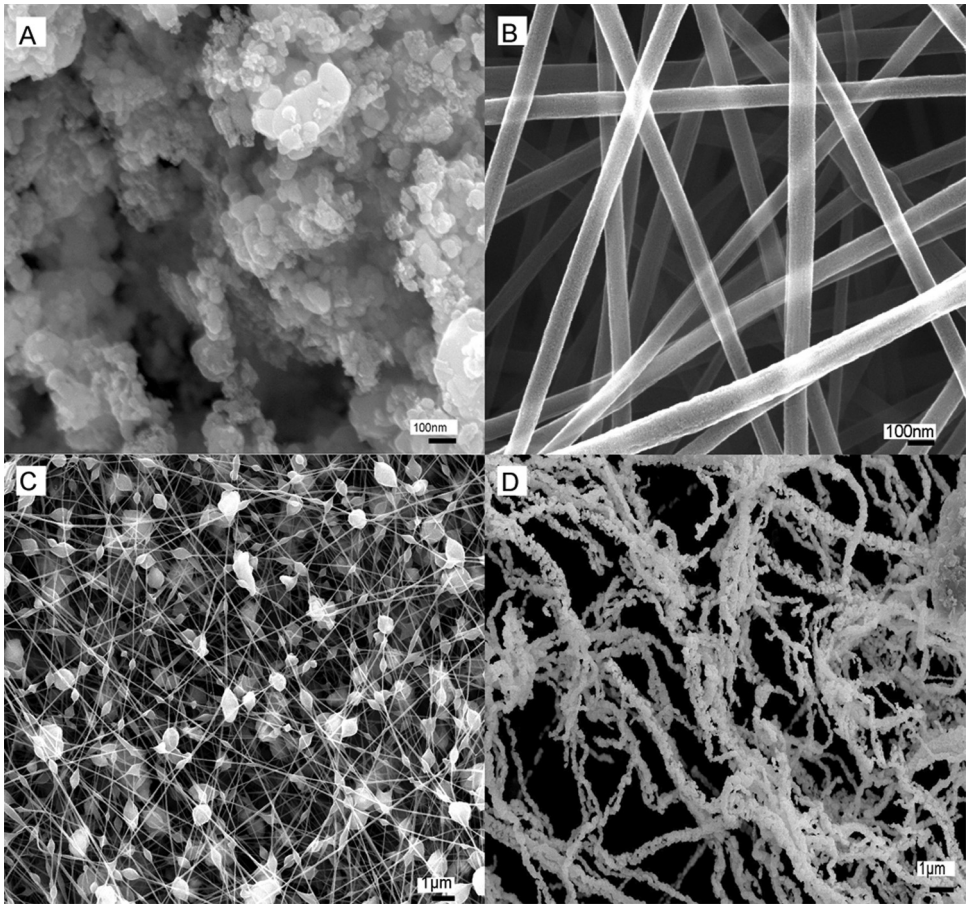

Fig. 2. SEM analysis of preparing CLL electrode. SEM images of (a) LFP particles, (b) CMC-Li nanofiber by electrospinning, (c) LFP/CMC-Li composite nanofiber by electrospinning, and (d) CLL composite nanofiber as electrode after carbonization at a high temperature.

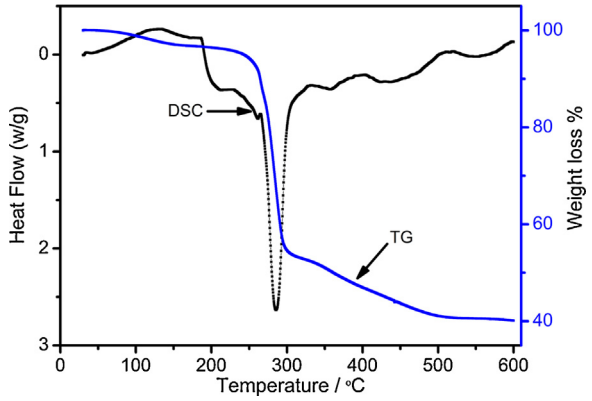

Fig. 3. TG–DSC results for LFP nano-fiber precursor in nitrogen. The figure shows maximum exothermic peak and the weight loss process appearing in temperature range and confirm the sintering temperature.

material is of significance to improve the capacity of the battery. Furthermore, the battery using CMC-Li with high DS has superior capacity and better electronic conductivity and electrochemical properties than that with low DS (Fig. 5).

3.6. The curves' analysis of CV with different materials

From Fig. 6, the positions of the oxidation–reduction peak of the dissimilar electrodes are distinctive. The difference in voltage between the two oxidation–reduction peaks of LFP electrode coated with CMC-Li by electrospinning should be less than that of

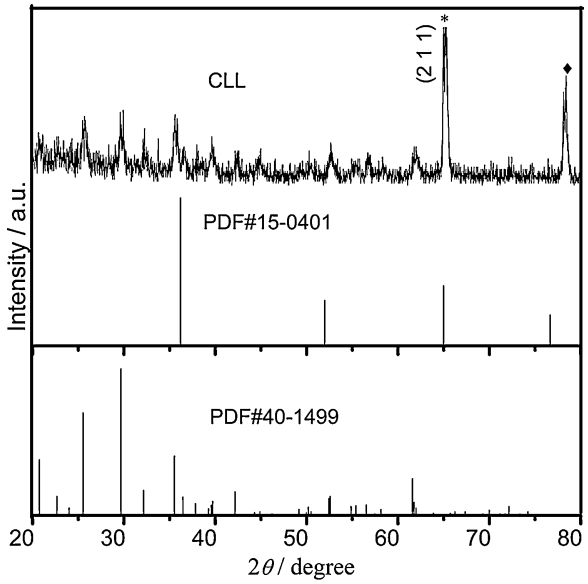

Fig. 4. X-ray diffraction crystal structure of electrode slice with CLL as cathode material (PDF#15-0401 is standard XRD of Li, PDF#40-1499 is standard XRD of LFP). CMC-Li modified cathode material maybe increase the contents of lithium ions in the whole battery, and improve the efficiency of prolapsing and embedding of lithium ions between cathode and anode electrode, thus, improving the diffusion efficiency and specific capacity.

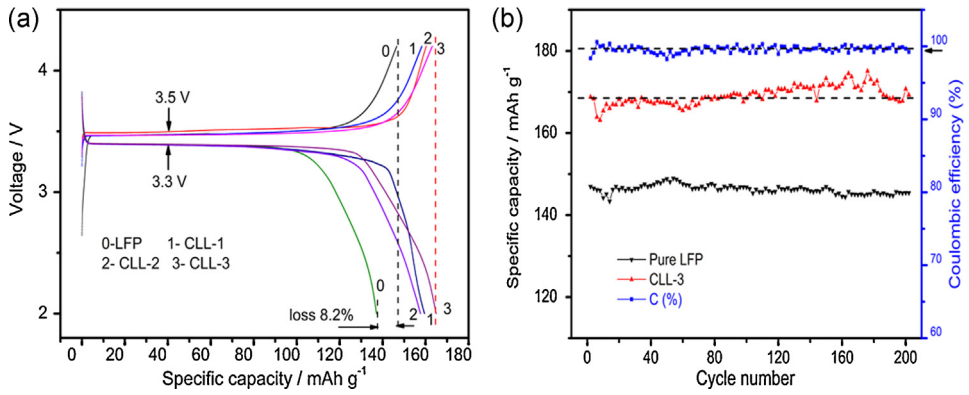

Fig. 5. The cycle comparison chart of the modified composite electrodes. (a) The first charge and discharge curves of different cathode material. (b) The charge specific capacity and efficiency of battery with CLL-3 and LFP as cathode material after 200 cycles. After 200 cycles, the least one is the battery with CLL-3 as electrode material, which is almost close to the zero and has the best performance cycles.

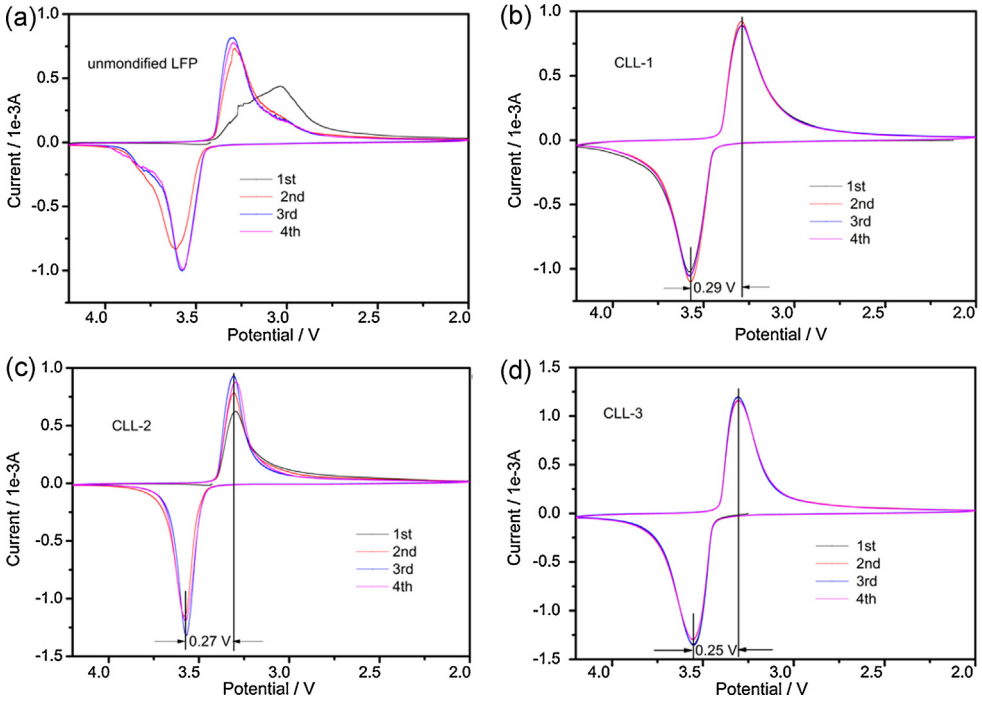

Fig. 6. CV tests of batteries with different electrode material. The distance between the discharge and charge curves of CLL is smaller than that of LFP, which shows that the polarization of the former is weaker than the latter and the difference of CLL and LFP electrode materials are 0.25 V and 0.68 V, respectively.

unmodified LFP. The CV curves of modified LFP electrodes are sharper than those of unmodified LFP. The distance between the discharge and charge curves of CLL is smaller than that of LFP, which shows that the polarization of the former is weaker than the latter and the difference of CLL and LFP electrode materials are 0.25 V and 0.68 V, respectively. This may be because the CLL particles were coated with the increase content of freely moving lithium ion to form an effective ionic-conductivity layer, which provided a diffusion pathway for Li^+ to reach the active particle surface, and it enhanced the activity of electrochemical reactions. CMC-Li with the high DS was superior to that with the low DS, and the lowest redox peak of the difference is 0. 25 V and the CLL electrode material polarization is weaker.

3.7. The curves' analysis of CV with different materials

Fig. 7 showed the EIS of electrode materials in the open state. Diameter size of the high-frequency semicircle reflected the size of

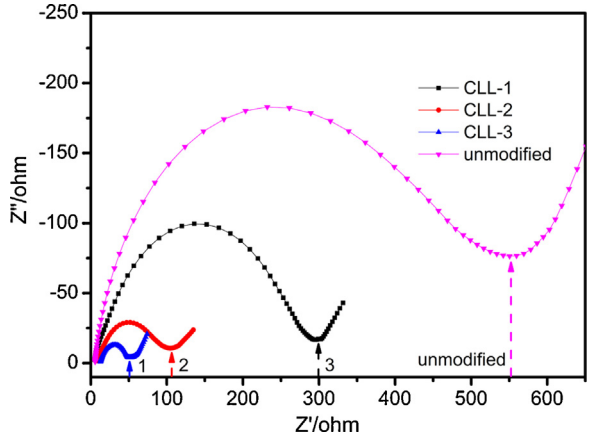

Fig. 7. The curves analysis of CV with different materials. These results indicated that the interfacial properties between LFP electrode and electrolyte were improved by using CNF/Li to increase the electrochemical reaction and dynamic performance. CNF/Li had played a positive role in the charge transfer process.

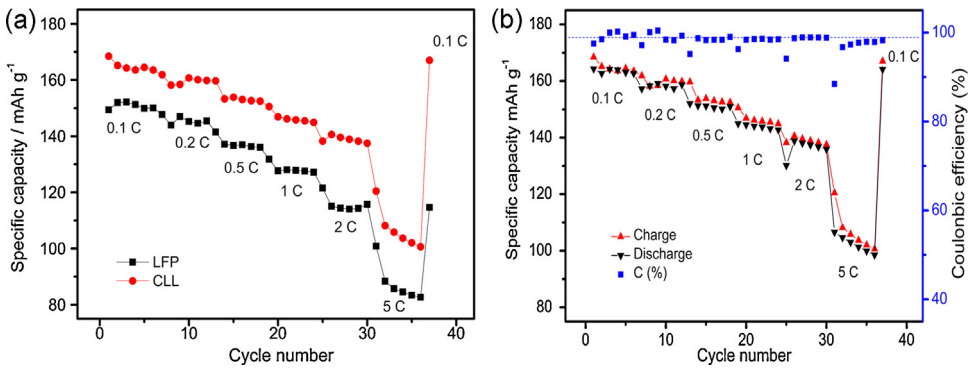

Fig. 8. The discharge/charge capacity cycle curves of cells with two electrode materials. (a) The curves of charge capacity at different rates for CLL and LFP as electrode materials. (b) The curves of discharge/charge capacity at the different rate for CLL as electrode materials. Such excellent rate performance strongly confirmed that it can not only enhance the cycle stability of material, but also improve the rate property of electrode materials by CLL modification with CMC-Li.

the charge transfer resistance of a cell. Obviously, the diameters of the semicircles in the high-frequency electrodes with LFP electrode material were bigger than those for the electrodes with CLL material. Compared with LFP, the charge-transfer resistance of a cell with CLL electrode was much lower. These results indicated that the interfacial properties between LFP electrode and electrolyte were improved by using CNF/Li to increase the electrochemical reaction and dynamic performance. CNF/Li played a decisive role in the charge transfer process. For CMC-Li with different DS, the polar group numbers carried by unit mass of CMC-Li with high DS were greater than those carried by CMC-Li with low DS. The repellency of CMC-Li with high DS was better, and the CLL layer formed on the active grain surface was more stable. The charge-transfer resistance of the cell using CMC-Li with high DS was obviously lower than that with low DS.

3.8. Curve analysis of charge/discharge rate and Coulomb efficiency

It could be seen from Fig. 8 that the rate performance and cycle property of electrode material with CLL-3 as electrode materials were excellent not only in small rate of charge and discharge but also in big rate of charge and discharge. As the discharge–charge rate increased from 0.1 C to 5 C, the discharge capacities of CLL demonstrated remarkable rate capability. Delivering discharge capacity of 168.5 mAh g^{-1}, 161.9 mAh g^{-1}, and 120.5 mAh g^{-1} at 0.1 C, 0.2 C and 5 C, respectively. As the discharge–charge rate decreased from 5 C to 0.1 C, capacity can be quickly approximate to its original level, which showed that the discharge capacity present linear variation with the increment of rate performance. Such excellent rate performance strongly confirmed that it can not only enhance the cycle stability of material, but also improve the rate property of electrode materials by CLL modification with CMC-Li. There may be two reasons, on one hand, it was because CNF/Li can be uniformly distributed in the surface of LFP material, the ionized Li-ions can shorten its transmission distance between cathode and anode electrode, and enhance the transmission efficiency and conductivity, which caused the material to have the relatively good rate performance and cycle property. On the other hand, ionic conductivity of LFP was related to the size of particles. The smaller the particle was, the shorter the transmission channel of lithium ion in LFP became. The faster lithium ion can come in and out, the better the property of the battery will be.

4. Conclusions

This study used cotton, as a raw material, synthesized novel functional materials water-soluble ionic cellulose derivative CMC-Li by a unique two-step method. Considering the characteristics of CMC-Li, for the first time, nano-CMC-Li fiber, CMC-Li/LFP and CLL composite nanometer fibers were successfully obtained by electrospinning. CLL was applied in Li-ion batteries increase the content of Li-ions in the entire batteries, and the material surface structure of the current collector is critical to achieve high electrode performance. The discharge platform of the battery was high, and the degree of polarization was small, which exhibited the excellent electrochemical performance. CMC-Li with the higher DS has better electrochemical performance than CMC-Li with the lower DS. Meantime, the CMC-Li is cheaper, more eco-friendly and easily degraded, safer, and it also applied in the field of other related materials.

Acknowledgements

Financial support from the special programs of graduate students' scientific and technological innovation activities of Beijing Institute of Technology (3090012241302) and Youth Science and Technology Innovation Projects of North Chemical Industry Co., Ltd. (QKCZ-BIT-04).

Appendix A. Supplementary data

Supplementary data associated with this article can be found, in the online version, at http://dx.doi.org/10.1016/j.carbpol.2014.03.052.

References

Blachechen, L. S., Souza, M. A., & Petri, D. F. S. (2012). Effect of humidity and solvent vapor phase on cellulose esters films. *Cellulose*, *19*(2), 443–457.
Cheng, C., & Fan, H. J. (2012). Branched nanowires: Synthesis and energy applications. *Nano Today*, *7*(4), 327–343.
Dimesso, L., Foerster, C., Jaegermann, W., Khanderi, J. P., Tempel, H., Popp, A., et al. (2012). Developments in nanostructured $LiMPO_4$ (M = Fe, Co, Ni, Mn) composites based on three dimensional carbon architecture. *Chemical Society Reviews*, *41*(15), 5068–5080.
Gibot, P., Casas-Cabanas, M., Laffont, L., Levasseur, S., Carlach, P., Hamelet, S., et al. (2008). Room-temperature single-phase Li insertion/extraction in nanoscale Li(*x*)FePO(4). *Nature Materials*, *7*(9), 741–747.
Gur, I., Sawyer, K., & Prasher, R. (2012). Searching for a better thermal battery. *Science*, *335*(6075), 1454–1455.
Hu, L.-H., Wu, F.-Y., Lin, C.-T., Khlobystov, A. N., & Li, L.-J. (2013). Graphene-modified $LiFePO_4$ cathode for lithium ion battery beyond theoretical capacity. *Nature Communications*, (4)
Janssen, Y., Santhanagopalan, D., Qian, D., Chi, M., Wang, X., Hoffmann, C., et al. (2013). Reciprocal salt flux growth of $LiFePO_4$ single crystals with controlled defect concentrations. *Chemistry of Materials*, *25*(22), 4574–4584.
Jiang, S. H., Duan, G. G., Schobel, J., Agarwal, S., & Greiner, A. (2013). Short electrospun polymeric nanofibers reinforced polyimide nanocomposites. *Composites Science and Technology*, *88*, 57–61.

Kuss, C., Lepage, D., Liang, G., & Schougaard, S. B. (2013). Ultrafast charging of $LiFePO_4$ with gaseous oxidants under ambient conditions. *Chemical Science*, *4*(11), 4223–4227.

Malik, R., Zhou, F., & Ceder, G. (2011). Kinetics of non-equilibrium lithium incorporation in $LiFePO_4$. *Nature Materials*, *10*(8), 587–590.

Marcicki, J., Canova, M., Conlisk, A. T., & Rizzoni, G. (2013). Design and parametrization analysis of a reduced-order electrochemical model of graphite/$LiFePO_4$ cells for SOC/SOH estimation. *Journal of Power Sources*, *237*, 310–324.

Moriwake, H., Kuwabara, A., Fisher, C. A. J., Huang, R., Hitosugi, T., Ikuhara, Y. H., et al. (2013). First-principles calculations of lithium-ion migration at a coherent grain boundary in a cathode material, $LiCoO_2$. *Advanced Materials*, *25*(4), 618–622.

Petrovic, M., Rakic, I. S., Runte, S., Busse, C., Sadowski, J. T., Lazic, P., et al. (2013). The mechanism of caesium intercalation of graphene. *Nature Communications*, *4*.

Qiu, L., Shao, Z., Liu, M., Wang, J., Li, P., & Zhao, M. (2014). Synthesis and electrospinning carboxymethyl cellulose lithium (CMC-Li) modified 9, 10-anthraquinone (AQ) high-rate lithium-ion battery. *Carbohydrate Polymers*, *102*, 986–992.

Qiu, L., Shao, Z., Wang, J., Zhang, D., & Cao, J. (2013). Study on synthesis rheological and electrospinning functional materials of carboxymethyl cellulose lithium (CMC-Li). *Acta Chimica Sinica*, *71*(11), 1521–1526.

Qiu, L., Shao, Z., Yang, M., Wang, W., Wang, F., Wan, J., et al. (2014). Study on effects of carboxymethyl cellulose lithium (CMC-Li) synthesis and electrospinning on high-rate lithium ion batteries. *Cellulose*, *21*(2), 615–626.

Qiu, L., Shao, Z., Yang, M., Wang, W., Wang, F., Xie, L., et al. (2013). Electrospun carboxymethyl cellulose acetate butyrate (CMCAB) nanofiber for high rate lithium-ion battery. *Carbohydrate Polymers*, *96*(1), 240–245.

Ritcharoen, W., Thaiying, Y., Saejeng, Y., Jangchud, I., Rangkupan, R., Meechaisue, C., et al. (2008). Electrospun dextran fibrous membranes. *Cellulose*, *15*(3), 435–444.

Rodriguez, K., Gatenholm, P., & Renneckar, S. (2012). Electrospinning cellulosic nanofibers for biomedical applications: Structure and in vitro biocompatibility. *Cellulose*, *19*(5), 1583–1598.

Ryou, M.-H., Kim, J., Lee, I., Kim, S., Jeong, Y. K., Hong, S., et al. (2013). Mussel-inspired adhesive binders for high-performance silicon nanoparticle anodes in lithium-ion batteries. *Advanced Materials*, *25*(11), 1571–1576.

Sasaki, T., Ukyo, Y., & Novak, P. (2013). Memory effect in a lithium-ion battery. *Nature Materials*, *12*(6), 569–575.

Stein, A. (2011). Energy storage batteries take charge. *Nature Nanotechnology*, *6*(5), 262–263.

Wang, J. L., & Wan, W. (2011). Combined effects of temperature and pH on biohydrogen production by anaerobic digested sludge. *Biomass & Bioenergy*, *35*(9), 3896–3901.

Wu, X.-L., Guo, Y.-G., Su, J., Xiong, J.-W., Zhang, Y.-L., & Wan, L.-J. (2013). Carbon-nanotube-decorated nano-$LiFePO_4$ @C cathode material with superior high-rate and low-temperature performances for lithium-ion batteries. *Advanced Energy Materials*, *3*(9), 1155–1160.

Xiong, M., Tang, H., Wang, Y., & Pan, M. (2014). Ethylcellulose-coated polyolefin separators for lithium-ion batteries with improved safety performance. *Carbohydrate Polymers*, *101*, 1140–1146.

Yang, Z., Zhang, J., Kintner-Meyer, M. C. W., Lu, X., Choi, D., Lemmon, J. P., et al. (2011). Electrochemical energy storage for green grid. *Chemical Reviews*, *111*(5), 3577–3613.

Yuan, J., Xu, Y., & Mueller, A. H. E. (2011). One-dimensional magnetic inorganic–organic hybrid nanomaterials. *Chemical Society Reviews*, *40*(2), 640–655.